

Original Article

Metabolism of esfenvalerate in tomato plants (*Solanum lycopersicum*)

Daisuke ANDO* and Takuo FUJISAWA

Environmental Health Science Laboratory, Sumitomo Chemical Co., Ltd., 4-2-1 Takarazuka, Hyogo 665-8555, Japan

(Received April 4, 2020; Accepted June 10, 2020)

The metabolic fate of esfenvalerate (**1**), ¹⁴C-labeled at the chlorophenyl or phenoxyphenyl ring, in tomato plants was investigated by spraying it three times at 15 g/ha. The overall metabolic trend of **1** was similar in foliage and fruit. The applied **1** gradually penetrated into the foliage/fruit, and approximately 30% of the total radioactive residue (TRR) distributed within the plant. The applied radioactivity remained mostly intact on the plant surface, while its degradation proceeded *via* ester cleavage to produce two corresponding acids derived from the chlorophenyl and phenoxyphenyl moieties, followed by saccharide conjugation at the inner tissues (each <5%TRR). While **1** retained its optical configuration (2*S*, α *S*) on the plant surface and in the fruit, a very slight isomerization at the α -cyanobenzyl carbon occurred to form a (2*S*, α *R*) isomer in the foliage (\leq 1%TRR). The isomerization at another asymmetric carbon C2 in the isovaleric acid moiety did not proceed on/in the plant for **1** or its metabolite.

Keywords: esfenvalerate, formulation, chiral pesticide, chiral metabolite, isomerization, plant metabolism.

Introduction

Esfenvalerate, **1** [(2*S*, α *S*)- α -cyano-3-phenoxybenzyl 2-(4-chlorophenyl)-3-methylbutyrate], is a synthetic pyrethroid known for its unique chemical structure of not having a cyclopropane ring, unlike typical pyrethroids,¹ and has been used worldwide to control a number of relevant insect species. While fenvalerate, the racemate of **1**, consists of four isomers (2*RS*, α *RS*) derived from the benzylic carbon in the chlorophenyl isovaleric acid moiety (2*RS*) and the α chiral center in the cyanobenzyl carbon of the phenoxybenzyl alcohol moiety (α *RS*), **1** has been solely designated to have a (2*S*, α *S*) configuration serving as a single chiral insecticide to provide the highest biological activity among its isomers.²

Generally, a pesticide is directly sprayed on crops to protect them from harmful pests, and therefore, the distribution and residual level of the chemical and its transformation products in agricultural commodities must be determined to estimate the pesticide-derived dietary burden for crop-consumer protection. In this respect, the implementation of a pesticide metabolism study in crop(s) using the radiolabeled test substance(s) is an initial and general approach for safety evaluation. In the past, the metabolic fate of **1** in cabbage, as well as fenvalerate and

(2*S*, α *RS*) isomers in cabbage, bean, and wheat, has been examined.³⁻⁶ The test results for the above three related substances showed very similar metabolic profiles in the plants, irrespective of their different combinations/ratios of the four isomers (2*RS*, α *RS*). Briefly, the pesticides gradually penetrated into the plant tissues and were mainly metabolized *via* hydrolysis of the ester linkage to produce the corresponding two carboxylic acids derived from the chlorophenyl and phenoxyphenyl rings, which both successively underwent phase II conjugation with various endogenous sugars. As minor pathways, hydroxylation at the 2- or 4-position of the phenoxy moiety, and hydration of the nitrile group to an amide with successive oxidation to carboxylic acid proceeded. In addition, a unique reaction, such as decarboxylation followed by C–C bond formation between the two chiral carbons, which was chemically demonstrated to be driven by the sunlight-induced cleavage of the ester or benzyl ether bond, was observed on the plant surface.⁷⁻¹⁰ Although each metabolic profile of four constituent isomers has not been individually examined, it is extremely important that **1**, fenvalerate, and (2*S*, α *RS*) isomers showed no stereoselective decomposition/metabolism on and in plants.³⁻⁶

Meanwhile, a draft guidance on risk assessment for plant protection products that contain stereoisomers has recently been issued by the EFSA (European Food Safety Authority, August 2019).¹¹ Based on the possibility that isomers can exhibit different bioactivity and degradation behavior in living organisms and environment, the EFSA document indicates the importance of evaluating the influence of each isomer for both the intact pesticide and its transformation products. Therefore, the isomeric profile of pesticides having asymmetric carbons has recently drawn much attention toward advanced risk characterization as an active research field.¹²⁻¹⁴ Therefore, we newly examined the

* To whom correspondence should be addressed.

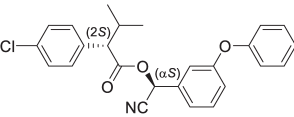
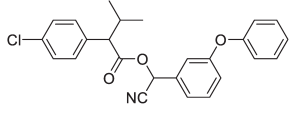
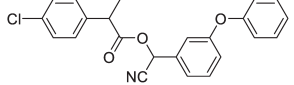
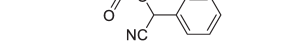

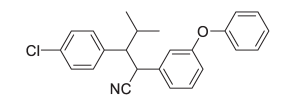
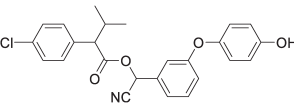
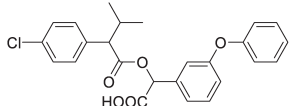
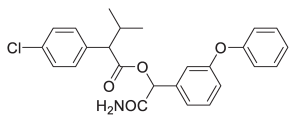
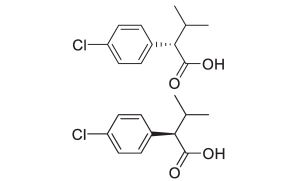
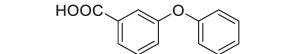
E-mail: andod@sc.sumitomo-chem.co.jp

Published online July 22, 2020

metabolic behavior of **1** sprayed onto tomato plants in accordance with representative agricultural use in the EU, namely, a 5% EC (emulsifier concentrate) formulation was applied three times at 15 g/ha with a 14-day interval during the growth stage BBCH (Biologische Bundesanstalt, Bundessortenamt und Chemische Industrie)¹⁵ 51 (inflorescence emergence) to 85 (fruit ripening), following the test guidelines for the study of pesticide metabolism in plant [OECD (Organisation for Economic Co-operation and Development) 501¹⁶] and OCSPP (Organization Chart for the Office of Chemical Safety and Pollution Preven-

tion) 860.1300¹⁷] to satisfy the global standard requirements for pesticide evaluation. In this study, the isomerization of not only **1** at the tomato plant surface and inner plant tissues but also a typical major metabolite, the chlorophenyl isovaleric acid derivative, generated *via* ester cleavage whose optical configuration at C2 carbon is originally in (*S*) form, was newly confirmed. In addition, various types of metabolite conjugation were determined using liquid chromatography–electrospray ionization–high-resolution mass spectrometry.

Table 1. Chemical structures of esfenvalerate, isomers and its metabolites/degradates

Compound	Structure	HPLC retention time (min)		TLC R_f value
		Reverse ^{a)}	Normal	
1		48.5	42.4 ^{b)}	0.76
Fenvalerate		48.5	46.5 ^{b)}	0.76
[2 <i>S</i> , α <i>S</i>]			43.3 ^{b)}	
[2 <i>R</i> , α <i>S</i>]			38.2 ^{b)}	
[2 <i>S</i> , α <i>R</i>]			35.0 ^{b)}	
2		47.4	—	0.75
		46.4		
3		40.3	—	0.56
4		42.6	—	0.24
5		38.9	—	0.30
		38.3		0.24
6		25.7	30.5 ^{c)}	0.48
			27.2 ^{c)}	
7		23.5	—	0.36

^{a)} Conventional analysis of metabolites (HPLC method 1). ^{b)} Chiral analysis of **1** isomers, *i.e.*, fenvalerate (HPLC method 3). ^{c)} Chiral analysis of **6** isomers (HPLC method 4).

Materials and Methods

1. Chemicals

Two kinds of ^{14}C -**1** uniformly radiolabeled at the chlorophenyl or phenoxyphenyl ring, abbreviated as CP-**1** (specific radioactivity: 4.47 GBq/mmol) and PP-**1** (4.51 GBq/mmol), were prepared in our laboratory (Sumitomo Chemical Company, Ltd., Osaka, Japan) and at Pharmaron UK, Ltd. (Cardiff, UK), respectively, according to the previous report.¹⁸⁾ The radiochemical purity of

each ^{14}C compound exceeded 99.0%. Non-radiolabeled reference standards **1**–**7**, listed in Table 1, were all prepared in our laboratory,^{3–5,7–10)} and their chemical purity was >70%. The emulsifier Sorpol 3544X, for preparing the EC formulation, was obtained from Toho Chemical Industry Co., Ltd. (Tokyo, Japan). All other reagents and solvents used in this experiment were of analytical grade or higher.

Table 2. ^{14}C distribution in tomato plant

	Chlorophenyl label					
	Foliage				Fruit	
	7 DAT		31 DAT		31 DAT	
	%TRR	ppm	%TRR	ppm	%TRR	ppm
Surface						
1	67.8	0.494	68.1	1.991	75.2	0.159
2	ND	ND	0.1	0.003	ND	ND
Extract						
1	25.4	0.185	25.4	0.731	16.6	0.035
6	ND	ND	0.7	0.019	0.3	<0.001
6 -Glc-Sul	1.2	0.008	2.0	0.057	1.7	0.004
6 -Glc-M	2.4	0.017	1.2	0.036	2.0	0.004
6 -Glc	0.8	0.006	0.7	0.024	0.3	<0.001
6 -2Glc	0.2	0.001	0.2	0.007	ND	ND
Others ^{a)}	ND	ND	0.2	0.006	0.6	0.001
Unextractables	2.2	0.016	1.3	0.038	3.3	0.007
Total	100.0	0.728	100.0	2.924	100.0	0.211

ND: Not detected. ^{a)} Consists of >2 components, 0.3%TRR as a single maximum. Sul: Sulfate. Glc: Glucose. M: Malonic acid.

	Phenoxyphenyl label					
	Foliage				Fruit	
	7 DAT		31 DAT		31 DAT	
	%TRR	ppm	%TRR	ppm	%TRR	ppm
Surface						
1	70.9	0.425	71.4	2.309	68.1	0.175
2	ND	ND	0.1	0.003	ND	ND
Extract						
1	21.7	0.130	18.1	0.585	25.5	0.065
4	0.3	0.002	ND	ND	0.3	<0.001
7	0.6	0.004	ND	ND	1.9	0.005
7 -Glc-M	1.9	0.011	1.3	0.042	1.2	0.003
7 -Glc	1.4	0.008	1.5	0.049	0.4	<0.001
7 -2Glc	0.2	0.001	0.8	0.026	ND	ND
Others ^{a)}	2.3	0.014	3.2	0.104	2.4	0.006
Unextractables	0.7	0.004	3.5	0.113	0.2	<0.001
Total	100.0	0.600	100.0	3.234	100.0	0.257

ND: Not detected. ^{a)} Consists of >5 components, 1.2%TRR as a single maximum. Glc: Glucose. M: Malonic acid.

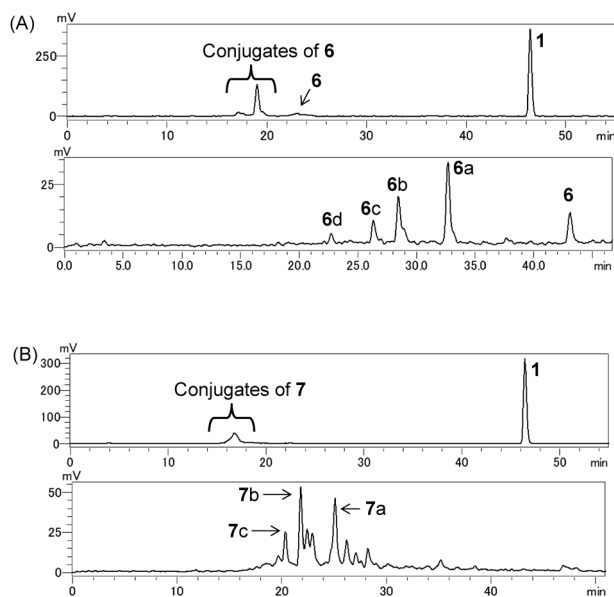


Fig. 1. Representative HPLC chromatograms of [CP-1] foliage 31 DAT (A) and [PP-1] foliage 31 DAT samples (B). Extracts (HPLC method 1, top), aqueous fractions (HPLC method 2, bottom). 6a: glucose sulfate conjugate; 6b: malonylglucose conjugate; 6c: glucose conjugate; 6d: diglucose conjugate; 7a: malonylglucose conjugate; 7b: glucose conjugate; 7c: diglucose conjugate.

2. Plant materials and ^{14}C treatments

Each tomato plant (*Solanum lycopersicum*, variety: Patio) was grown in a Wagner pot filled with Kasai soil (Hyogo, Japan) in a greenhouse under the natural sunlight at 24°C during the day and 21°C at night. The plant treatment was conducted following the representative agricultural use in the EU. Based on the typical application rate for the tomato plant, 15 g/ha per spray, and the estimated circular cultivation area of the pot, 2000 cm² (diameter *ca.* 50 cm), the target application amount was proportionally calculated to be 300 μg per plant. Each 300 μg of ^{14}C -1 was mixed with 5.7 mg of EC blank formulation (Solpol 3554X/xylene=11.1/88.9, w/w) in a 20 mL atomizer bottle on the day of the application and uniformly dispersed in 15 mL of deion-

ized water in accordance with the actual spray volume of 500–1200 L/ha. After analyzing the aliquot *via* liquid scintillation counting (LSC), the dose solution in the atomizer was evenly sprayed onto each plant. In total, three spray applications were conducted, on June 19, July 3, and 17, 2019, in the same manner at 14-day intervals during the growth stages of the test plants at BBCH 51 to 85. After each spray, the inner bottle was rinsed with acetone, and the remaining ^{14}C was quantified *via* LSC to accurately calculate the radioactivity sprayed onto each tomato plant. The recovered radioactivity was thereafter analyzed *via* HPLC (methods 1 and 3) to evaluate the stability of 1 during the spray application.

3. Analytical procedures

For intermediate sampling, three tomato leaves were collected 7 days after the first treatment (DAT) using scissors. For final sampling, each whole mature plant was harvested by cutting the plant stem just above the soil at 31 DAT, *i.e.*, 3 days after the third application. The mature tomato plant was separated into fruit and foliage. All samples were weighed and surface-rinsed by immersing into acetonitrile in beakers. The rinsed foliage was frozen at -80°C and pulverized, and a 20 g aliquot was extracted with 100 mL of acetone/water (2/1, v/v) at 10,000 rpm and 0°C for 10 min using a homogenizer AM-8 (Nissei, Ltd., Osaka, Japan). The homogenate was vacuum filtered to separate the extract and plant residue. The residue was extracted twice in the same manner, and the filtrate was combined. Three tomato fruits were directly extracted with 100 mL of acetone/water (2/1, v/v) per fruit, followed by filtration similarly to the foliage samples for a total of three times. Each aliquot of the surface rinse and acetone/water extract was analyzed *via* LSC to quantify the radioactivity and then subjected to HPLC and TLC analyses on the same day of the sampling. The unextractables (plant residues) were air-dried and individually combusted for LSC analysis. All of the extracts were stored in a freezer ($<4^\circ\text{C}$) until use in further analyses. The total radioactive residue (TRR) in each plant was determined as a sum of ^{14}C in the surface rinse, extract, and unextractable residue.

Table 3. The list of mass spectrometric data of conjugated metabolites

	Identity	m/z	Formula	Δ ppm	RDB ^{a)}
Chlorophenyl- ^{14}C					
6-Glc-Sul	[6+Glc+Sul] ⁻	453.0630 (457.0553)	C ₁₇ H ₂₀ O ₁₀ ³⁵ Cl ³² S (C ₁₇ H ₂₀ O ₁₀ ³⁷ Cl ³⁴ S)	+0.776 -0.447	6.5 6.5
6-Glc-M	[6+Glc+M-H] ⁻	461.1224	C ₂₀ H ₂₆ O ₁₀ ³⁵ Cl	+0.894	7.5
6-Glc	[6+Glc+HCOO] ⁻	419.1130	C ₁₈ H ₂₄ O ₉ ³⁵ Cl	+1.376	6.5
6-2Glc	[6+2Glc+HCOO] ⁻	581.1651	C ₂₄ H ₃₄ O ₁₄ ³⁵ Cl	+1.228	7.5
Phenoxyphenyl- ^{14}C					
7-Glc	[7+Glc+H] ⁺	377.1241	C ₁₉ H ₂₁ O ₈	+0.130	9.5
7-Glc-M	[7+Glc+M+H] ⁺	463.1248	C ₂₂ H ₂₃ O ₁₁	+0.400	11.5
7-2Glc	[7+2Glc+HCOO] ⁻	583.1677	C ₂₆ H ₃₁ O ₁₅	+1.503	11.5

Sul: Sulfate, Glc: Glucose, M: Malonic acid. RDB: Ring and double bond equivalents

4. Chromatography

The test substance and its metabolites were analyzed *via* high-performance liquid chromatography (HPLC). A reversed-phase HPLC system consisted of a Shimadzu LC module (LC-20A series, Shimadzu Co., Ltd., Kyoto, Japan) equipped with a Sumipax ODS A-212 column (5 μ m, 6 mm i.d. \times 15 cm, Sumika Chemical Analysis Service, Ltd., Osaka, Japan). The following gradient system was employed as a conventional method to analyze **1** and its metabolites (method 1) at a flow rate of 1 mL/min: 0.1% formic acid (Solvent A) and acetonitrile (Solvent B), 0–5 min, %A/%B (v/v), 100/0; 10 min, 50/50; 25 min, 35/65; 50 min, 0/100; 50.1–55 min, 100/0. The radioactivity in the column eluent passed through a UV detector was measured using a Flow Scintillation Analyzer Radiomatic 150TR radiodetector (PerkinElmer, Co., Tokyo, Japan) equipped with a 500 mL liquid cell using Ultima-Flo AP[®] (PerkinElmer, Co.) as a scintillator. To separate the conjugate metabolites generated in the plant, an additional gradient was applied (method 2): 0–5 min, %A/%B (v/v), 100/0; 10 min, 75/25; 15 min, 60/40; 40 min, 0/100; 50.1–55 min, 100/0. The chiral analysis of **1** with normal-phase HPLC was conducted using a Sumichiral OA 2000 column (5 μ m, 4 mm i.d. \times 25 cm, Sumika Chemical Analysis Service, Ltd.) mounted in a Shimadzu column oven CTO-20AC at 30°C with an isocratic eluent of *n*-hexane/isopropanol (500/1, v/v) at a flow rate of 1.0 mL min⁻¹ (method 3). The stereo form of **6** was confirmed using a Daicel Chiralcel OD-H column (5 μ m, 4 mm i.d. \times 25 cm; Daicel Co., Ltd., Tokyo, Japan) maintained at 30°C with *n*-hexane/ethanol/trifluoroacetic acid (300/1/0.05, v/v/v) at a flow rate of 1.0 mL/min (method 4). Thin-layer chromatography (TLC) was carried out for an analytical purpose using a precoated silica gel 60F₂₅₄ thin-layer chromatoplate (20 \times 20 cm, 0.25 mm thick, Merck Millipore, Darmstadt, Germany). The solvent system applied was toluene/ethyl acetate/acetic acid, 75/25/1 (v/v/v). The nonradiolabeled reference standards were detected by exposing the chromatoplate to ultraviolet light. An autoradiogram was prepared by transcribing the TLC plate to a BAS-III Fuji Imaging Plate (Fuji Photo Film Co., Ltd., Tokyo, Japan) for several hours. The radioactivity in each spot exposed on the imaging plate was detected by a Bio-Imaging Analyzer Typhoon (GE Healthcare, Tokyo, Japan). The typical HPLC retention times and *R_f* values of **1** and the related reference standards are summarized in Table 1.

5. Radioanalysis

The radioactivity in the plant surface rinses and extracts was determined *via* LSC with a Packard Model 2900TR spectrometer (Packard Instrument Co., Inc., Illinois, US) after mixing each aliquot with 10 mL of PerkinElmer Emulsifier Scintillator Plus[®]. The plant residues after extraction (unextractables) were combusted using a PerkinElmer Model 307 sample oxidizer. The ¹⁴CO₂ produced by the procedure was trapped into 9 mL of PerkinElmer Carb[®]-CO₂ absorber and mixed with 15 mL of PerkinElmer Permafluor[®] scintillator, and then the radioactivity therein was quantified using LSC. The combustion efficiency was determined to be greater than 92.9%.

6. Mass spectroscopy

Liquid chromatography–electrospray ionization–high-resolution mass spectrometry (LC–ESI–HRMS) analysis of the metabolites was conducted using a Q-Exactive Focus (Thermo Fisher Scientific Inc., Tokyo, Japan) mass spectrometer equipped with the same HPLC instruments/radiodetector modules described in the chromatography section, *i.e.*, LC-20A and 150TR modules. The gradient system employed was HPLC method 2. The analytical parameters at the mass module controlled by the Xcalibur software (version 2.2) were as follows: sweep gas flow 10 unit, source temp. 100°C, desolvation temp. 350°C, capillary voltage 3.5 kV, cone voltage 10–40 eV, resolution 70,000 FWHM (full-width at half maximum), mass range 100–1000 *m/z*. MS/MS analysis was implemented with stepped collision energies at 10, 15, and 20 eV. The HPLC column eluent was divided in half, and equal amounts were introduced to the mass spectrometer and radiodetector.

7. Identification/characterization of radioactive components

The identity of **1** and its metabolites was confirmed by HPLC and TLC cochromatographies with the reference standards, in which the corresponding retention times and *R_f* values of ¹⁴C components and standards, respectively, were compared. In order to characterize unknown polar metabolites in the samples, each plant extract was partitioned with *n*-hexane to remove **1** from the remaining aqueous fraction. The LC–HRMS analysis was implemented for each aqueous layer using HPLC method 2 to obtain the chemical structure information on the unknowns. The characteristic isotopic pattern of the carbon atom inherited from the radiolabeling of the intact CP-**1** or PP-**1** was traced to distinguish the mass spectrum of each metabolite from abundant plant matrices. In addition, inclusion of chlorine and sulfur atoms was inspected by their natural isotopic distributions. Furthermore, MS fragmentation patterns were investigated in detail to support the metabolite characterization.

8. Chiral analysis

In the pretreatment for the chiral analysis of **1** recovered by the surface rinse and extraction, each aliquot was dried with a stream of nitrogen for the surface rinse fractions, while the one of extract was evaporated to remove acetone, partitioned using hexane, and the organic fractions was dried under nitrogen. Subsequently, they were redissolved in *n*-hexane/isopropanol (500/1, v/v) and directly injected into the chiral HPLC system (method 3). For metabolite **6**, the metabolite was isolated from the extract by HPLC fractionation (method 2) and evaporated/dried in vacuum, followed by reconstitution in *n*-hexane/ethanol/trifluoroacetic acid (300/1/0.05, v/v/v), and then subjected to the chiral analysis (method 4). In addition, the chirality of **6** conjugated with malonylglucose, as a representative major conjugate, was confirmed in the same manner after deconjugation by the following acid hydrolysis: 1.0 mL of 6.0 M HCl was added to the HPLC-isolated conjugate (approximately 20,000 dpm), dried in a vial, and refluxed at 100°C for 6 hr with stirring.

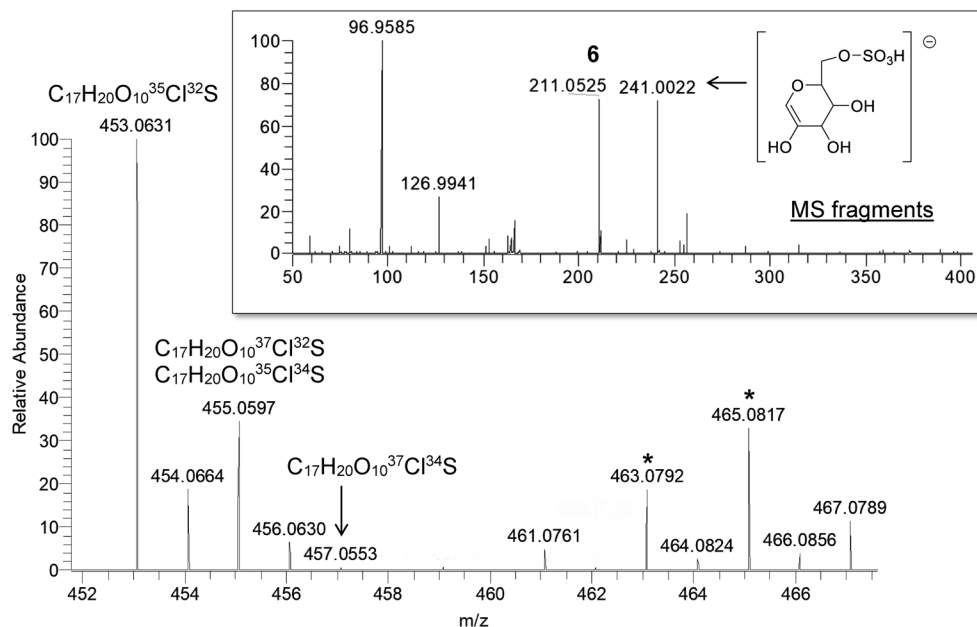


Fig. 2. Mass spectra of the glucose sulfate conjugate of **6**. Elemental compositions of choline and sulfur isotopic combinations are shown on the corresponding signals. Asterisks show $^{14}\text{C}_5$ and $^{14}\text{C}_6$ isotopic peaks. Note that the orbitrap applied in this study had insufficient resolving power (resolution 70,000 FWHM) to separate $^{37}\text{Cl}^{32}\text{S}$ and $^{35}\text{Cl}^{34}\text{S}$ signals; however, a $^{37}\text{Cl}^{34}\text{S}$ peak was clearly distinguished.

After neutralization using 12.0 M NaOH, the released **6** was purified by HPLC and subjected to the chiral analysis.

Results

1. ^{14}C Spray application

The radioactivity sprayed onto plant in each and the total of three applications ranged from 99.5–116.8 and 102.3–103.7% of the nominal target ratio, respectively. The ^{14}C component in the dose solution remained in the atomizer bottle after each spray application was confirmed by HPLC analysis, and the only radioactive component detected was the intact **1** retaining a (2S, α S) configuration, showing its stability in the EC formulation during the treatment.

2. ^{14}C Distribution and residue in tomato plants

The total ^{14}C recovered from the mature tomato plant, *i.e.*, leaf/ foliage and fruit, was 88.3 and 87.0% of the applied radioactivity for the CP and PP label, respectively. The ^{14}C distributions in tomato plants are shown in Table 2. The profile of the radioactivity recovered from the surface and inner portion of the plants was similar between the CP and PP labels. The radioactivity detected in the surface rinse was 67.8–71.4% TRR for leaves (7 DAT) and foliage (31 DAT), and 68.1–75.2% TRR for fruit, which showed the same trend regardless of the different sampling points or plant portions. In the surface rinse fraction, **1** was the only component detected except for 31 DAT foliage, where **2** existed at an extremely low level (0.1% TRR). For the extract, **1** remained as the most abundant ^{14}C residue (16.6–25.5% TRR), with multiple minor metabolites for both radiolabels. In the CP label-treated samples, the maximum amount of free form **6** accounted for

0.7% (31 DAT, foliage) and its total sum, *i.e.*, free and conjugated forms, 4.8% TRR (31 DAT, foliage). The major metabolite detected in the PP label-treated plants was **7**, which existed as free form for 1.9% TRR (31 DAT, fruit), and its total sum was 4.1% TRR (7 DAT, foliage). Metabolite **4** was also observed at $\leq 0.3\%$ TRR (7 DAT, foliage; 31 DAT, fruit) as a minor one. For both radiolabels, several other ^{14}C components were detected but were insignificant, as each one was below 1.2% TRR. The unextractables in both foliage and fruit were $< 3.5\%$ TRR, and therefore no further analyses were conducted.

3. Identification/characterization of metabolites

The chemical structures of **2**, **4**, **6**, and **7** were identified using HPLC and TLC cochromatographies with the synthetic reference standards. For both radiolabels, all of the unknown metabolites, which did not match any of the standards, remained in the aqueous layer after partitioning of the plant extracts with hexane indicated the water-soluble characteristic. In conjunction with the high polarity compared to the typical metabolites **6** and **7**, as shown by the earlier HPLC retention times (Fig. 1), the unknowns were deduced to be their conjugates. To confirm this assumption, LC-HRMS analyses have been conducted and, as a result, the chemical structures of major unknown metabolites were clarified to be mono-/disaccharides and malonylglucose conjugates of **6** and **7**, and glucose sulfate conjugate of **6**, as summarized in Table 3. For the detail, all of the molecular-related ions derived from each metabolite were determined by the radioisotopic pattern elicited from the ^{14}C labeling at each aromatic ring of **6** and **7** ($^{14}\text{C}_6/^{14}\text{C}_5/^{12}\text{C}_1 = 3/2/10$) and the chlorine atom of **7** ($^{37}\text{Cl}/^{35}\text{Cl} = 1/3$). For the structure of the glucose

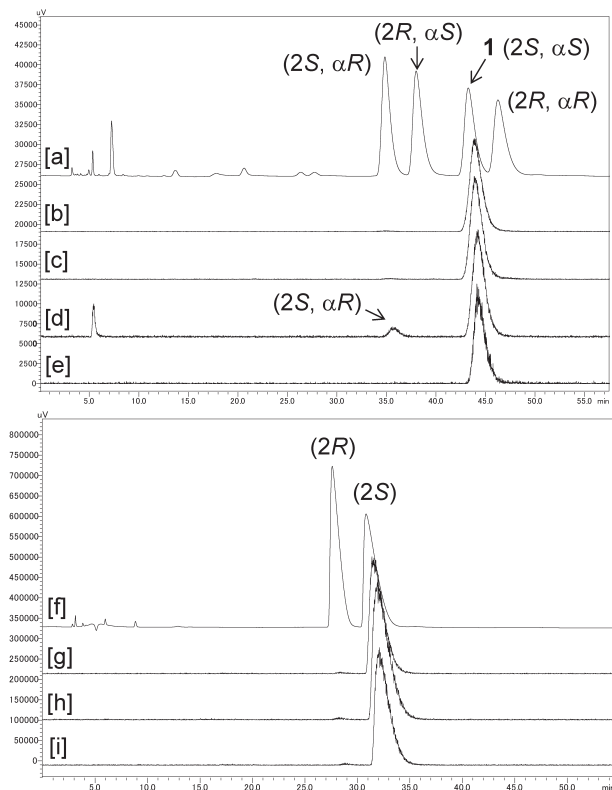


Fig. 3. Representative chiral HPLC chromatograms of **1** (top) and metabolite **6** (bottom), at Day 31, chlorophenyl label. [a]: Reference standards of **1** isomers (fenvalerate); [b]: **1** on the foliage surface; [c]: **1** on the fruit surface; [d]: **1** in the foliage extract; [e]: **1** in the fruit extract; [f]: reference standard of **6** (*R/S*); [g]: **6** in the foliage extract; [h]: **6** in the fruit extract; [i]: deconjugated **6** obtained from the malonylglucoside in fruit extract. The identity of each ^{14}C peak was confirmed by cochromatography with corresponding reference standards for each chiral HPLC analysis.

sulfate conjugate of **6**, the existence of a sulfur atom was additionally confirmed by the presence of the isotopic combinations ($^{37}\text{Cl}^{34}\text{S}/[^{37}\text{Cl}^{32}\text{S} + ^{35}\text{Cl}^{34}\text{S}]/^{35}\text{Cl}^{32}\text{S} = 1/22/57$, theoretical ratio), as depicted in Fig. 2. The candidate chemical formula from the m/z

of the molecular-related ion was filtered by relative mass deviation ($\Delta < |5|$ ppm from the theoretical values for each metabolite, with additional inspection of the given unsaturated degrees and ^{13}C isomer content. Furthermore, the MS fragmentation profile was fully investigated and showed a characteristic peak of m/z 211.0526 eq to that of **6** ($\text{C}_{11}\text{H}_{11}\text{O}_2^{35}\text{Cl}$, $\Delta -3.178$ ppm) in the negative ion mode for each conjugate of the CP label and m/z 197.0597 for the dehydrate of **7** ($\text{C}_{13}\text{H}_9\text{O}_2$, $\Delta -2.814$ ppm) in the positive ion mode for conjugates of the PP label, which clearly suggested their aglycones should be considered as **6** and **7**, respectively. For further confirmation, the malonylglucose of **6** detected in the fruit aqueous extract was isolated and hydrolyzed in the acidic condition, and the chemical structure of the released aglycone was determined *via* HPLC and TLC cochromatographies with the reference standard.

4. Chiral analysis

The chiral HPLC analysis of **1** collected from the surface rinses of foliage and fruit showed a single peak corresponding to the (*2S,αS*) configuration throughout the cultivation period, which suggested that the original optical form was maintained on the plant surface (Fig. 3). Meanwhile, **1** distributed in the foliage extract underwent a very slight isomerization to a (*2S,αR*) isomer $\leq 1.0\%$ TRR, whilst the test substance in the fruit retained its chirality. No isomerization at the C2 carbon of the isovaleric acid moiety was observed for **1** on/in the tomato plant. With respect to the free form **6** generated in the foliage and fruit, the absolute configuration at the asymmetric C2 was demonstrated to maintain the (*2S*) form (Fig. 3). The geometry of **6** released from the malonylglucose conjugate in fruit by the acid hydrolysis was additionally investigated and, likewise, was confirmed to be a (*2S*) isomer only.

From the overall results, the fate of **1** in the tomato sprayed with the EC formulation is proposed in Fig. 4.

Discussion

The ^{14}C recovery by the surface wash exceeded 67% of the ap-

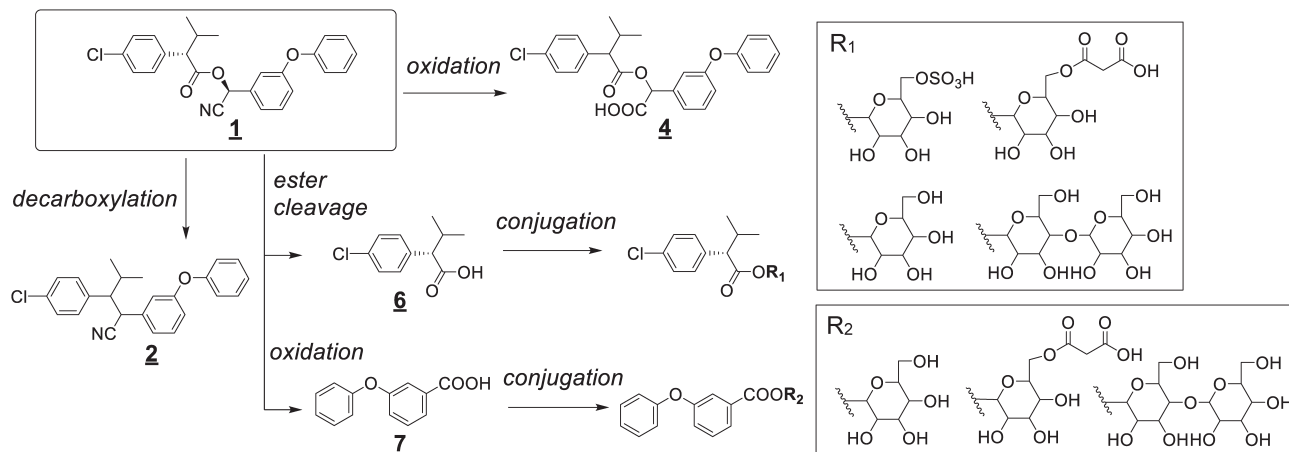


Fig. 4. Proposed metabolic pathway of **1** in tomato plants. R_1 : endocons of **6**; R_2 : endocons of **7**.

plied radioactivity throughout the incubation, which may indicate that the major portion of ^{14}C that remained on the plant surface had been exposed to sunlight. The photolytic degradation of **1** is known to proceed very rapidly, with a degradation half-life of 0.5–1.0 days, which produces multiple degradates in solution or clay suspensions,¹⁰ and this has been considered a critical environmental factor for the dissipation of **1** from crops.^{3,4,6} In contrast, photo-rearranged/decarboxylated product **2** was the only degrade slightly detected in the surface rinse within this study, and notably, its production ratio was much lower than the one reported in the previous plant metabolism study.³ Furthermore, no photolysis-enhanced isomerization of **1**⁶ was observed for the surface fraction. Taking all of the above into consideration, although the majority of **1** likely remained in the vicinity of the plant surface after spray application, it was considered that immediate penetration of **1** into the wax layer or cuticle proceeded to mitigate the sunlight exposure or to scavenge the light energy from surrounding plant materials.¹⁹ In addition, the adjuvants in formulation, which was not used in the previous study,⁶ likely operated as a synergetic factor for assisted penetration of **1** and the photolysis suppression.^{20–22}

With respect to the metabolic reactions, the ester hydrolysis of **1** proceeded almost simultaneously with oxidation at the benzyl carbon of the phenoxyphenyl ring to produce **6** and **7** as major phase I modifications. In general, an ester bond is labile in living organisms, for example, majority of pyrethroids^{23–26} as well as organophosphates, carbamates,^{25,26} and proherbicide esters²⁷ are known to receive cleavage as an initial major reaction typically mediated by esterase,^{25–28} *i.e.*, a biotic reaction, and also by hydrolysis, *i.e.*, abiotic reaction. In reference to the reported acidic pH of the tomato homogenate, *ca.* 4–5,²⁹ irreversible deesterification was not expected to be promoted; however, the reaction was supposed to be driven in an alkaline region such as phloem (pH 7–8)³⁰ or in the presence of catalytic biomolecules to enhance cleavage, as observed in the hydrolysis study with clay minerals.¹⁰ Subsequent to phase I, various phase II conjugations were likely initiated by glucosidation for both **6** and **7**. These phase I/II reactions were consistent with the metabolic pathway previously reported for **1** and fenvalerate in plants,^{3–6} except for the sulfate glucose conjugation observed in our tomato study. Although the conjugate was newly characterized for **1**, sulfation on xenobiotics has been reported in diverse flora such as *Arabidopsis thaliana*,³¹ cotton,³² radish, spinach, and lettuce³³; thus, this type of reaction was considered one of the important enzymatic detoxifications of xenobiotics in plants, similar to that known in mammals,³⁴ fish, and invertebrates^{35–37} that extensively utilize sulfate-accompanying conjugation in their detoxification responses.

In this study, though at an insignificant ratio, the isomerization of **1** at the cyano-connecting asymmetric carbon in foliage was newly demonstrated. The observed stereo-conversion was not unexpected, taking into account the chemical nature of **1** harboring an α -cyanobenzyl chiral carbon. For example, the isomerization at the α -cyanobenzyl has been reported for

1 as well as for cypermethrin and cyfluthrin in water at a neutral pH, while permethrin and bifenthrin, possessing no cyano group did not receive the chiral conversion, indicating the involvement of cyano-induced deprotonation followed by electric resonance with neighboring carbonyl and re-protonation at the α -cyanobenzyl carbon as a general base catalysis mechanism.^{10,38,39} In conjunction with the result that no sunlight-induced isomerization on the tomato surface was observed, it was presumed that $(2S,\alpha S) \rightarrow (2S,\alpha R)$ proceeded by the base-catalytic chemical reaction. Alternatively, catalysis by racemase or epimerase could intervene in isomerization as a general enzymatic pathway,⁴⁰ but such a possibility was not confirmed and requires further examination. On the other hand, no isomerization at C2 of the acid moiety of **1** or **6** proceeded in our study. Likewise, with the exception of deltamethrin, epimerization at the tertiary C2 of the chrysanthemic acid moiety of various pyrethroids in solution has not been reported in hydrolysis or chiral stability studies, and this was considered to be due to the insufficient acidity of the chiral methine proton or to less accessibility to the base molecule due to steric hindrance.^{39,41–44} In comparison with general chrysanthemic moieties, the acidity of the C2 proton of **1** and **6** could be reinforced somewhat to give a corresponding carbanion intermediate through aromatic resonance stabilization,⁴⁴ but it was considered that the corresponding proton was still unlikely to be reactive enough, and/or the hydrogen-subtraction was hampered by adjacent bulky functions (*t*-butyl, aromatic ring, and carbonyl), for isomerization.

In conclusion, we confirmed the fate of **1** sprayed with an EC formulation on tomato plants. The effect of the formulation on the behavior of **1** was assumed to be the enhancement of penetration into the plant to suppress sunlight-induced mineralization/dissipation. The metabolic pathway in the plant was similar to that in previous reports, except for glucose sulfate conjugate detected. The isomeric composition of **1** in the plant (foliage) was newly confirmed, and we found a slight $(2S,\alpha S) \rightarrow (2S,\alpha R)$ isomerization at the cyanobenzyl chiral carbon, which was likely to be driven by a chemical base-catalytic reaction, while the absolute configuration at C2 of the carbonyl moiety thoroughly retained a (2S) form for **1** and its metabolite **6**.

References

- 1) N. Ohno, K. Fujimoto, Y. Okuno, T. Mizutani, M. Hirano, N. Itaya, T. Honda and H. Yoshioka: *Agric. Biol. Chem.* **38**, 881–883 (1974).
- 2) K. Aketa, N. Ohno, N. Itaya, I. Nakayama and H. Yoshioka: *Agric. Biol. Chem.* **42**, 895–896 (1978).
- 3) N. Mikami, N. Wakabayashi, H. Yamada and J. Miyamoto: *Pestic. Sci.* **16**, 46–58 (1985).
- 4) H. Ohkawa, K. Nambu and J. Miyamoto: *J. Pestic. Sci.* **5**, 215–223 (1980).
- 5) N. Mikami, N. Wakabayashi, H. Yamada and J. Miyamoto: *Pestic. Sci.* **15**, 531–542 (1984).
- 6) P. W. Lee, S. M. Stearns and W. R. Powell: *J. Agric. Food Chem.* **36**, 189–193 (1988).
- 7) N. Mikami, N. Takahashi, H. Yamada and J. Miyamoto: *Pestic. Sci.* **16**, 101–112 (1985).

- 8) N. Mikami, N. Takahashi, K. Hayashi and J. Miyamoto: *J. Pestic. Sci.* **5**, 225–236 (1980).
- 9) Y. Suzuki and T. Katagi: *J. Agric. Food Chem.* **56**, 10811–10816 (2008).
- 10) T. Katagi: *J. Agric. Food Chem.* **41**, 2178–2183 (1993).
- 11) EFSA (European Food Safety Authority) L. Bura, A. Friel, J. O. Magrans, J. Parra-Morte and C. Szentes : *EFSA J.* **17**, 5804 (2019).
- 12) N. C. P. Albuquerque, D. B. Carrao, M. D. Habenschus and A. R. M. Oliveira: *J. Pharm. Biomed. Anal.* **147**, 89–109 (2018).
- 13) X. Zhang, X. Wang, F. Luo, H. Sheng, L. Zhou, Q. Zhong, Z. Lou, H. Sun, M. Yang, X. Cui and Z. Chen: *Ecotoxicol. Environ. Saf.* **172**, 530–537 (2019).
- 14) I. J. Buerge, A. Bächli, R. Kasteel, R. Portmann, R. López-Cabeza, L. F. Schwab and T. Poiger: *Environ. Sci. Technol.* **53**, 5725–5732 (2019).
- 15) U. Meier (ed.): “Growth Stages of Mono- and Dicotyledonous Plants; BBCH Monograph,” Federal Biological Research Centre for Agriculture and Forestry: Berlin, Germany, pp 120–123, 2001.
- 16) OECD: *OECD Guidelines for the Testing of Chemicals 501, Metabolism in Crops* (2007).
- 17) EPA: *Residue Chemistry Test Guidelines, OCSPP 860.1300 Nature of the Residue-Plants: Livestock* (1996).
- 18) H. Kanamaru, T. Kamada, I. Nakatsuka, Z. Mori, T. Okamura and I. Yoshitake: *J. Labelled Comp. Radiopharm.* **18**, 1283–1293 (1981).
- 19) T. Katagi: *Rev. Environ. Contam. Toxicol.* **182**, 1–189 (2004).
- 20) T. Katagi: *Rev. Environ. Contam. Toxicol.* **194**, 71–177 (2008).
- 21) A. M. Faers and R. Pontzen: *Pest Manag. Sci.* **64**, 820–833 (2008).
- 22) D. MacLachlan and D. A. Hamilton: *Pest Manag. Sci.* **67**, 609–615 (2011).
- 23) J. P. Demoute: *Pestic. Sci.* **27**, 375–385 (1989).
- 24) J. E. Casida and L. O. Ruzo: *Pestic. Sci.* **11**, 257–269 (1980).
- 25) C. E. Wheelock, G. Shan and J. Ottea: *J. Pestic. Sci.* **30**, 75–83 (2005).
- 26) I. R. Montella, R. Schama and D. Valle: *Mem. Inst. Oswaldo Cruz* **107**, 437–449 (2012).
- 27) M. Gershater, K. Sharples and R. Edwards: *Phytochemistry* **67**, 2561–2567 (2006).
- 28) B. Siminzsky: *Phytochem. Rev.* **5**, 445–458 (2006).
- 29) M. A. Bridges and M. R. Mattice: *Am. J. Dig. Dis.* **6**, 445–458 (2006).
- 30) P. White: “Marschner’s Mineral Nutrition of Higher Plants,” ed. by P. Marschner, Elsevier Ltd. Amsterdam, pp. 49–70, 2012.
- 31) Q. Fu, Q. Ye, J. Zhang, J. Richards, D. Borchardt and J. Gan: *Environ. Pollut.* **222**, 383–392 (2017).
- 32) T. M. Capps, V. M. Barringer, W. J. Eberle, D. R. Brown and F. R. Sanson: *J. Agric. Food Chem.* **44**, 2408–2411 (1996).
- 33) S. Pascal-Lorber, S. Despoux, E. Rathahao, C. Canlet, L. Debrauwer and F. Laurent: *J. Agric. Food Chem.* **56**, 8461–8469 (2008).
- 34) F. C. Kauffman: *Drug Metab. Rev.* **36**, 823–843 (2004).
- 35) D. Schlenk, M. D. Celander, E. Gallagher, S. George, M. James, S. Kullman, P. van den Hurk and K. Willett: “The Toxicology of Fishes,” eds. by R.T. Di Giulio and D.E. Hinton, CRC Press, Boca Raton, FL, pp. 153–234, 2008.
- 36) D. R. Livingstone: *Comp. Biochem. Physiol.* **120**, 43–49 (1998).
- 37) Y. Ikenaka, H. Eun, M. Ishizaka and Y. Miyabara: *Aquat. Toxicol.* **80**, 158–165 (2006).
- 38) W. Liu, S. Qin and J. Gan: *J. Agric. Food Chem.* **53**, 3814–3820 (2005).
- 39) T. Katagi: *J. Pestic. Sci.* **37**, 1–14 (2012).
- 40) M. E. Tanner: *Acc. Chem. Res.* **35**, 237–246 (2002).
- 41) B. Testa, P. A. Carrupt and J. Gal: *Chirality* **5**, 105–111 (1993).
- 42) C. Pepper, J. H. Smith, K. J. Barrell, P. J. Nicholls and M. J. Hewlins: *Chirality* **6**, 400–404 (1994).
- 43) J. R. Maguire: *J. Agric. Food Chem.* **38**, 1613–1617 (1990).
- 44) M. B. Smith and J. March: “March’s Advanced Organic Chemistry. Reactions, Mechanisms, and Structure,” 5th Ed., A Wiley-International Publication, John Wiley & Sons, New York, 2001.